Powering OMNI: A Distributed and Modular Closed-Loop Neuromodulation Device

George Alexandrov

Electrical Engineering and Computer Sciences
University of California at Berkeley

Technical Report No. UCB/EECS-2018-14
http://www2.eecs.berkeley.edu/Pubs/TechRpts/2018/EECS-2018-14.html

May 1, 2018

Powering OMNI: A Distributed and Modular Closed-Loop Neuromodulation Device

by George Alexandrov

Research Project

Submitted to the Department of Electrical Engineering and Computer Sciences, University of California at Berkeley, in partial satisfaction of the requirements for the degree of **Master of Science, Plan II**.

Approval for the Report and Comprehensive Examination:

Committee:

Jan Rabaey
Research Advisor

Date

* * * * * *

Elad Alon
Second Reader

Date

Abstract

Neurological disorders like Major Depressive Disorder (MDD) and Generalized Anxiety Disorder (GAD) broadly affect a billion people worldwide. Despite the prevalence and debilitating effects of these disorders, there is no cure and treatment relies on chemical interventions that are oftentimes ineffective. In the last decade, deep brain stimulation (DBS) has emerged as an effective solution for the symptomatic treatment of movement disorders such as Parkinson's Disease, Essential Tremor, and Dystonia, and recent research has demonstrated the potential of DBS and closed-loop neuromodulation in also treating some neuropsychiatric disorders. Unlike movement disorders, neuropsychiatric disorders manifest in the brain at the systems level, necessitating a distributed, network approach to treatment that acts in closed-loop and responds in real time. To achieve this, a more sophisticated system than the current state-of-the-art is required in order to address disorders that manifest in complex neural pathways and affect physically distant regions of the brain.

Here we present the Octopus Mimetic Neural Implant (OMNI), a distributed and modular neuromodulation device capable of treating a variety neurological disorders. OMNI supports simultaneous recording and stimulation on up to 256 channels from up to 4 physically distinct neuromodulation modules placed cortically or sub-cortically around the brain. OMNI's unique distributed architecture and powerful embedded processing offers the capability to address disorders presented at the network level and enables a new class of closed-loop neuromodulation therapies.

The focus of this work is the power management and distribution network required for proper and safe operation of OMNI. Unlike existing neuromodulation systems, OMNI must provide power to a distributed and variable number of sub-modules, each with potentially different power dissipation. This huge load variation, combined with medical implant regulations which require implanted wires to carry no DC current, presents a unique challenge in powering OMNI. To address this problem, a power distribution network is presented which is comprised of a pair of power drivers that adaptively generate differential, constant voltage, variable power 20 MHz AC voltage waveforms.

Contents

List of Figures

List of Tables

1 Introduction

1.1 Neurological Disorders

Neurological disorders affect billions of people worldwide and account for between 4.5% and 10.9% of the global burden of disease [1], yet are some of the least understood disorders due to the complexity of the human brain. The most prevalent disorders are Major Depressive Disorder (MDD) and Generalized Anxiety Disorder (GAD), which affect 6.7% and 3.1% of Americans respectively [2]. Furthermore, MDD and GAD often co-occur with other illnesses such as cancer, diabetes, and Parkinson's Disease, and are common in patients who undergo prolonged hospital stays [3]. Despite the strong prevalence of these debilitating disorders, treatment options are imprecise and universally ineffective.

Current treatments for MDD and GAD target specific neurotransmitter receptors in the brain - serotonin, norepinephrine, and dopamine. Prozac and Zoloft, the most popular antidepressants, target specific chemical pathways in the brain in an effort to suppress depression. Unfortunately the chemical pathways that are involved in depression also play a much larger role in the human brain, leading to a plethora of side effects caused by antidepressant drugs. These can range from headaches and nausea to insomnia and an increased risk of seizures. In order to treat these disorders more safely and successfully, this chemical approach to treatment must be replaced with a comprehensive and targeted electrical one.

While there is currently no commercial neuromodulation device for treating MDD or GAD, there are a number of existing research and commercial devices for the treatment of movement disorders, another class of disorders affecting neural circuitry [4, 5]. One treatment that has proven to be effective in treating motor disorders such as Parkinson's Disease, Essential Tremor, and Dystonia is Deep Brain Stimulation (DBS), which works by applying stimulation at a specific brain target (typically a deep lying one such as the thalamus or subthalamic nucleus) in order to desynchronize abnormal oscillatory activity of neurons in that region [6]. While recent research has demonstrated the potential for DBS to treat depression and Post-Traumatic Stress Disorder (PTSD) [7, 8], current neuromodulation devices are inadequate for the treatment of neurological disorders that manifest in complex neural pathways and affect physically distant regions of the brain. In order to study, treat, and potentially cure disorders like MDD, GAD, and PTSD, a distributed neuromodulation device is required which acts in closed-loop and responds in real-time.

1.2 Existing Neuromodulation Systems

Current research and commercial devices for the treatment of movement disorders and epilepsy such as Medtronic's Activa PC+S [4] and NeuroPace's RNS System [5] rely on specific anatomical targets and electrode placement for stimulation. More importantly, these devices are housed in a central hub with long leads connecting electrodes to recording and stimulation circuitry. This configuration limits the number of recording/stimulation channels to a small number per device, since each channel needs a corresponding wire from electrode to hub, reducing cable flexibility and increasing size and tissue displacement.

This thesis presents an overview of a wireless, fully implantable neuromodulation system called Octopus Mimetic Neural Implant (OMNI) that is a distributed, modular, intelligent, and efficient approach to treating neurological disorders. These four properties make the system a perfect candidate for studying and treating neurological disorders. Distributed electronics allow easy access to physically distinct regions of the brain; modularity allows for easy configuration of the number and location of implants; intelligence allows for closed-loop operation that makes treatment possible; and efficiency ensures that the system is fully-implantable and can operate with a single Li-ion battery. A comparison of OMNI with current state-of-the-art commercial neuromodulation devices can be seen in Table 1.1. As can be seen, OMNI drastically improves on the recording and stimulation capabilities of existing systems while providing processing capable of running advanced algorithms for closed-loop neuromodulation.

This thesis focuses on one of the main challenges in implementing the OMNI system - providing safe and reliable power to all components. Unlike existing neuromodulation systems where all electrical components are housed in a central hub, OMNI utilizes a distributed and modular architecture that requires a drastically different approach to power distribution. The next chapter describes the OMNI system in more detail, including each sub-module. The challenges of powering such a system are then detailed, followed by a discussion on the design, implementation, and experimental results of the proposed solution to this problem.

Specification	**OMNI (this work)**	**Activa PC+S [4]**	**NeuroPace RNS [5]**
Number of electrode arrays	4 (any combination of cortical/subcortical)	2 (any combination of cortical/subcortical)	2 (1 cortical, 1 sub-cortical)
Number of channels	256	8	8
Recordable channels	256 channels simultaneously	Maximum of 2	Each channel selectable
Sampling rate	1000 Hz	200-800 Hz	200-600 Hz
Stimulators per array	4	1	1
Algorithms supported	Feature extraction, artifact elimination, MPC	SVM (Linear Kernel, 4DOF)	N/A
Real time telemetry	2 Mbps	11.7 kbps	N/A

Table 1.1: Comparison between this work and existing state-of-the-art neuromodulation systems.

2 The Octopus Mimetic Neural Implant (OMNI) System

The Octopus-Mimetic Neural Implant (OMNI) was developed as part of DARPA's Systems-Based Neurotechnology for Emerging Therapies (SUBNETs) project. It is funded by the BRAIN initiative which is set up with the goal of better understanding the human brain. The OMNI device brings together expertise from a wide array of backgrounds and was developed in collaboration with UC Berkeley, Cortera Neurotechnologies, and Lawrence Livermore National Laboratory (LLNL). The following sections describe the device as a whole, as well as the hardware in detail.

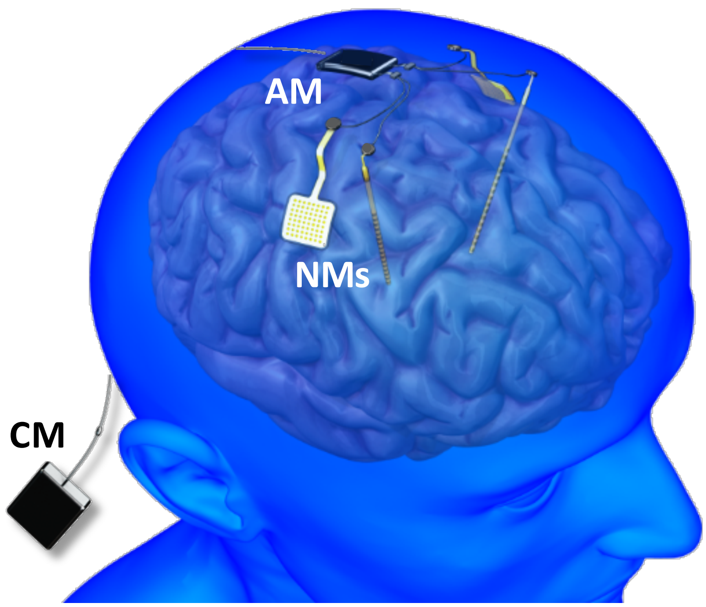

Figure 2.1: The OMNI device showing multiple NMs attached to the AM, sitting on the skull, where data and commands are multiplexed. The CM (shown here externally) is implanted in the chest cavity and is responsible for controlling and powering all sub-modules.

OMNI consists of three main types of modules, as seen in Figure 2.1. The Neuromodulator Modules (NMs) are "smart electrodes," each of which are comprised of a high-density thin-film electrode array integrated with a single custom low-power application specific integrated circuit (ASIC). The ASIC records and digitizes the neural signals at each electrode and sends the data in packets across a cable to a central router on the skull called the Aggregator Module (AM). The AM serializes and packetizes data from up to 4 NMs (easily scalable to 8) and sends it through a single cable to the main processor of the device called the Control Module (CM). The CM is implanted in the chest cavity and performs advanced processing on the received data and determines stimulation locations and parameters. It then sends stimulation commands to the AM, which routes them to the desired NMs. This architecture enables advanced closed-loop neuromodulation in a highly scaled and distributed manner.

2.1 Neuromodulation Module (NM)

The OMNI Neuromodulation Module Integrated Circuit (NMIC) is a 64-channel ASIC designed by Cortera Neurotechnologies. It is capable of simultaneous recording and stimulation on all 64 channels through 4 independent, highly-configurable stimulation units. AC power and data is provided through a custom 6-wire interface. It is compatible with both cortical and sub-cortical arrays, supports chronic and acute implantation, and allows for closed-loop neuromodulation. Figure 2.2 shows the NMIC and supported electrode arrays.

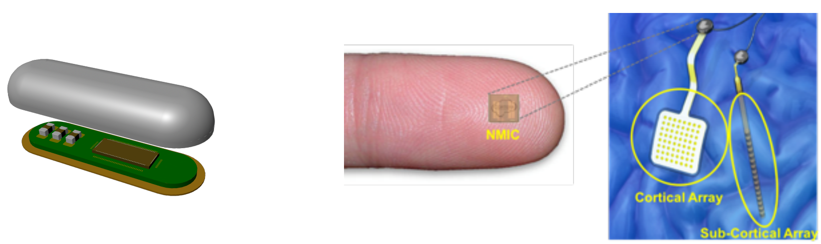

(a) (b)

Figure 2.2: (a) Model of NMIC and custom package and (b) cortical and sub-cortical electrode arrays supported by the NM.

The NMs enable various advancements of OMNI, most important of which is the reduction of interconnect complexity. As mentioned before, current commercial devices like the Activa PC+S and RNS contain all electronics in a central hub with long electrode leads extending to target areas around the brain. This configuration requires a separate wire for each electrode between the electrode array and device in order to transmit the recorded neural signals. Thus, as the number of recording channels is increased the diameter of the cable, volume of displaced tissue, and cross-talk between signal wires increases proportionally, effectively limiting the number of recording channels per site to around 10. Furthermore, the stimulation hardware is also far away from the electrodes, meaning that high voltage stimulation pulses must be routed through long cables.

OMNI addresses both of these issues through the NM's unique digital interface, which digitizes and packetizes neural data at the electrode interface and sends this data across a much smaller 6-wire cable to a central processor. This digital interface reduces the number of wires required per NM from over 70 to only 6 and enables multiple NMs to be implanted in the brain without displacing a large amount of brain tissue.

2.2 Aggregator Module (AM)

The Aggregator Module (AM) is a router of power and data signals to/from the CM and NMs. Figure 2.3a shows the block diagram of the AM which highlights its key components. An on-board IGLOO nano FPGA performs the low level mux/demux logic required to multiplex commands and data to/from the CM and NMs, while the data receivers ensure that the AC-coupled data signals are recovered correctly. While the AM is electrically simple, consisting mainly of an IGLOO nano FPGA, its operation is crucial to the OMNI system. It supports up to 4 NMs (scalable to 8) and 1 CM through a custom digital protocol. Custom DBS-style connectors designed by LLNL make system modularity possible by allowing an arbitrary and scalable number of neural interfaces to be plugged in. This functionality places the final design decision in the hands of the neurosurgeon, who can choose how many, what types, and where to place the NMs based on the patient's specific symptoms. Electrically, the AM acts as a multiplexer that routes command packets from a single CM to any configuration of up to 4 NMs as well as sending data packets in the other direction. Its custom protocol supports up to 8 NMs talking to a single CM and is the primary enabler of OMNI's modularity. Additionally, the AM has the ability to electrically disconnect any NM from the rest of the system in case of failure. This ability ensures that the rest of the OMNI system is not compromised in the event of a malfunctioning NM, electrode array, or cable. The AM is packaged in a custom hermetically sealed package as shown in Figure 2.3b and sits subcutaneously on top of the skull.

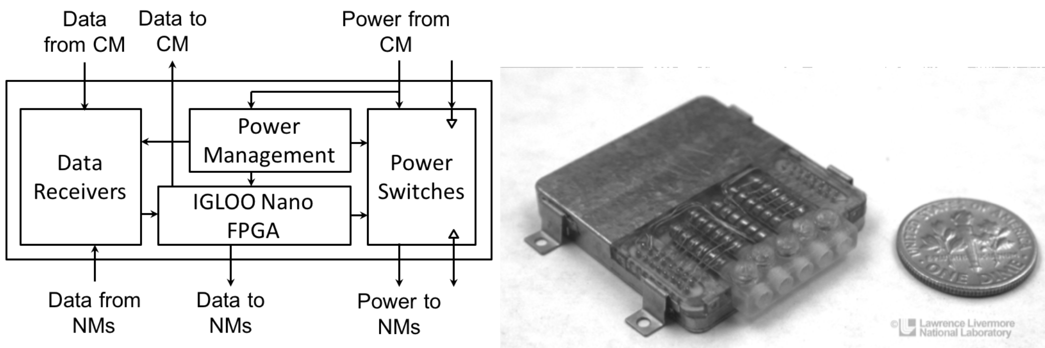

(a) (b)

Figure 2.3: (a) Block diagram showing the main sub-blocks of the AM, and (b) custom AM package with dime for size comparison.

2.3 Control Module (CM)

The Control Module (CM) is an integrated and programmable data processing, storage, and telemetry module implanted in the chest. It acts as the brain of system, controlling all sub-components and performing the computations required for closed-loop treatment. Figure 2.4a shows the block diagram of the CM, which consists of 4 main parts: power management, processing, storage, and telemetry. The CM PCB is housed in a hermetically sealed custom package designed by LLNL that includes an on/off switch and battery charger inputs and can be seen in Figure 2.4b.

2.3.1 Power Management

The CM is responsible for powering every other part of OMNI and is therefore one of the most important parts of the system. The CM contains a single $600\,\mathrm{mA\,h}$ Li-ion battery with a nominal voltage of $3.6\,\mathrm{V}$ that can power OMNI for 12-24 hours depending on usage scenarios. There are 3 regulators that step this battery voltage down to $2.5\,\mathrm{V}$, $1.8\,\mathrm{V}$, and $1.2\,\mathrm{V}$ for the various components on the CM. Unfortunately, due to medical implant regulations that require implanted wires to carry zero DC current, the AM and NMs cannot be powered through these same DC supplies. Instead, the CM generates AC power through a pair of differential AC power drivers whose design, implementation, and testing will be discussed in detail in Chapter 4.

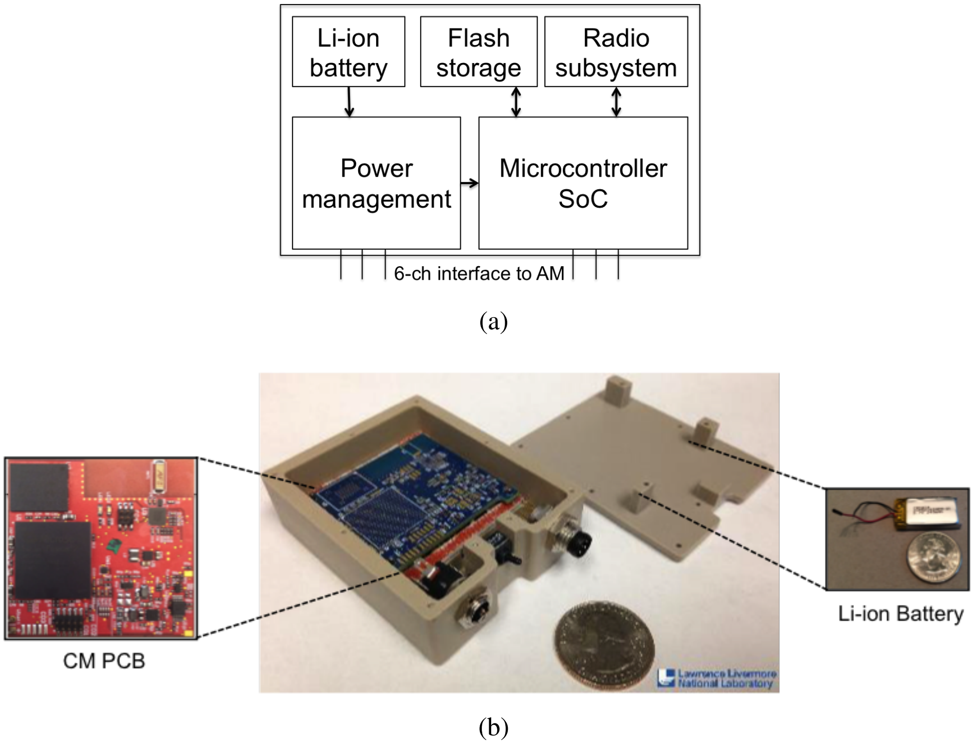

Figure 2.4: (a) Block diagram showing the main sub-blocks of the CM, and (b) custom CM package with PCB and battery.

2.3.2 Processing

The CM houses a Microsemi SmartFusion2 SoC - an advanced processing module comprised of an FPGA and ARM Cortex M3 processor in the same fabric. It is responsible for performing the necessary computations to enable real-time closed-loop operation, including FFTs, PCA, and linear control. While the algorithms required to effectively perform closed-loop neuromodulation are not covered in detail in this report, the design of the processing hardware in the CM was motivated by these requirements.

2.3.3 Telemetry and Storage

In order to support real-time wireless streaming of the large amount of data generated by OMNI's recording subsystem, the CM houses a Nordic nRF51822 $2.4\,\mathrm{GHz}$ radio running a custom communication protocol. The Nordic radio is capable of data rates of up to 2 Mbps, although numbers closer to $1.8\,\mathrm{Mbps}$ were measured due to packet overhead. This data rate supports full streaming (raw neural data) of up to 100 channels, or compressed streaming (e.g. energy binning) of all 256 channels for open-loop operation and data logging. The CM additionally houses a $4\,\mathrm{Gb}$ NAND Flash memory for local storage of data.

2.4 Cables and Connectors

The cables and connectors are a combination of custom and commercial provided by LLNL which support the distributed and modular nature of the OMNI system. As shown in Figure 2.5, the cables consist of 6 conductors arranged around a central twisted-pair (shown here as a single wire) in a multi-lumen configuration. This cable design minimizes cross-talk and noise while keeping cable thickness minimized. They are responsible for reliably carrying AC power and data to the AM and a configurable number of NMs, and are thus an integral part of the hardware design of the CM. While the design and implementation of these cables is not the focus of this work, their role in the design of the power network will be discussed in greater detail in Chapter 3.

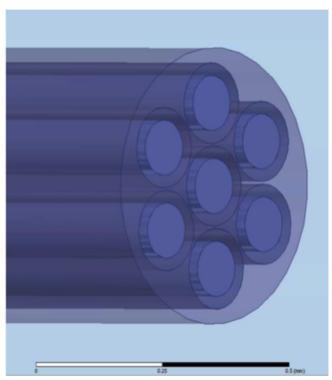

Figure 2.5: Multi-lumen cable used to connect NMs to AM and AM to CM

2.5 User Interface

A custom graphical user interface (GUI) was created for programming OMNI and is shown in Figure 2.6. This Python based software allows the user to read and write NM hardware registers, record real-time neural data, and set up stimulation waveforms in order to operate the device in

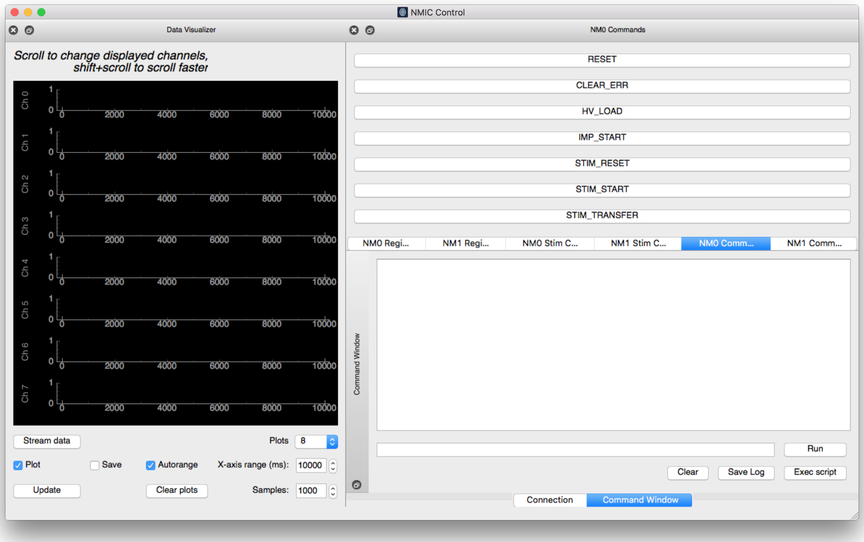

Figure 2.6: The graphical user interface for the OMNI system allows users to easily operate the device in open-loop mode and set up closed-loop operation.

open-loop mode. This allows a clinician to test OMNI during and after implantation in order to ensure that all parts of OMNI operate correctly before the surgical site is closed. Additionally, the GUI allows a user to configure all parameters of the system prior to closed-loop operation of OMNI.

3 The Power Problem

A major problem in any power distribution network is dealing with transient changes in loading from internal effects like changes in mode of operation and external factors like temperature. A power distribution network must deliver enough energy to its sub-blocks in order to power them reliably, while at the same time prevent excess power delivery which could cause heating, component damage, and failure. In a typical embedded device, power is derived from a single source (e.g. battery or capacitor) and distributed as DC power using one or more voltage regulators which provide a nearly ideal constant-voltage, variable-current source. Unfortunately, medical implant regulations require any implanted cable to carry zero DC component in order to prevent permanent tissue damage caused by harmful electrical fields generated within the body. This restriction means that while there can be DC voltages inside each hermetically sealed implanted module, any wires that pass through tissue must be AC coupled. Based on these regulations, OMNI is designed to generate differential AC power signals from a battery in the CM and distribute these through a pair of wires to the AM and NMs. In order to ensure safety and reliability of OMNI, these power drivers must operate efficiently and reliably across a wide range of operating conditions and loads, as well as ensure patient safety in the event of a device failure. Here we will outline some of the challenges inherent in such a system from both a circuit and system perspective.

3.1 RC Model of OMNI load

Figure 3.1 shows the RC model of the load that a CM must drive. There are four components of the power network: power driver, AM load, NM load, and interconnects. The power driver, modeled here as an ideal AC source for simplicity, is comprised of a pair of differential Class-E power drivers housed in the CM and will be discussed in detail in Section 4. The design of this power driver scheme is motivated by the rest of the network seen in Figure 3.1, the most important of which are the AM and NM loads. Again for simplicity, they are modeled as a full-wave diode rectifier and a simple RC load. Completing the connections between each module is a custom wire bundle consisting of 6 wires. There are 5 total cables in the system - one connecting the CM to the AM and 4 connecting the AM to the NMs. The AM also contains a bank of power switches that are responsible for disconnecting unused or malfunctioning NMs from the rest of the system (not shown here). The details of these sub-modules and their effects on the design of the power will be discussed next.

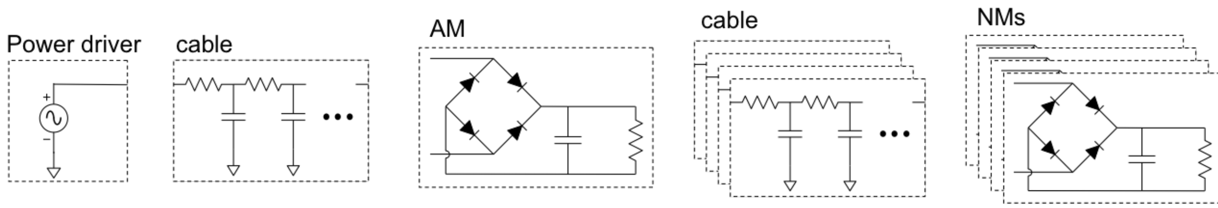

Figure 3.1: RC model of the load that the CM power drivers must drive. Connections between modules are not explicitly shown.

3.2 Variable Load

The main challenge in the design of the power drivers comes from the variable power requirements of the sub-modules. In a typical use case for OMNI, a patient will have one CM, one AM, and between one and four NMs connected. These NMs can change operating modes many times a minute, with each operating mode (on vs. off, recording vs. stimulating) requiring a different amount of power. The power driver must be able to supply both the minimum and maximum power and everything in between at a high efficiency in order to maximize operating lifetime of OMNI. The minimum power requirement of the device is determined solely by the AM and corresponds to an OMNI configuration with no NMs powered (e.g. during surgery when a clinician must connect the CM and AM to test basic functionality). In this case, the required power is

$$P_{min} = P_{AM} = 2\,\mathrm{mW}.$$

On the opposite extreme, the maximum power is determined by an OMNI configuration with an AM and 4 NMs which are constantly stimulating with all 4 stimulators. In this case,

$$P_{max} = P_{AM} + 4P_{NM,max} = 14\,\mathrm{mW}.$$

Note that in any configuration, the CM draws no power from the power drivers as it is DC powered directly from the battery. Accounting for various external factors and the overall efficiency of the power network, these power drivers must be able to operate with output power of $2\,\mathrm{mW}$ to $20\,\mathrm{mW}$. More importantly, this output power requirement is not fixed but changes with the use case and mode of operation of the device. For instance, in a typical application of OMNI a patient may have 2 NMs which record neural signals from 2 different regions of the brain. Based on the information contained within these neural recordings, the OMNI device may choose to apply stimulation at both NMs for a period of a few hundred milliseconds, after which it will continue solely recording. In this simplified example, the power required by the system can change from a few milliwatts to a few tens of milliwatts and back in under a second, and the power drivers must adapt to these changes in real-time. Thus, OMNI's AC power drivers must be intelligent and adaptive.

3.2.1 Constant Voltage or Constant Current?

In order to provide variable output power, OMNI must be able to adjust either its output voltage or output current in response to a changing load impedance. While both are feasible solutions, OMNI generates constant-voltage variable-current power signals in order to maximize the efficiency of the NMs, which are specifically designed to operate with maximum efficiency for a particular range of input voltages. This work will not go into detail on the internal circuitry of the NMs, but they contain RF-DC converters at their inputs that are optimized for input voltages of around $3.3\,\mathrm{V_{pp}}$. Since the NMs also account for a majority of the AC power dissipation (the AM only consumes around $2\,\mathrm{mW}$), the efficiency of their power train should be maximized by supplying them with AC inputs around $3.3\,\mathrm{V_{pp}}$. As will be seen in the following section, the power drivers achieve this by utilizing a voltage feedback loop in order to generate a constant output voltage with variable current (power).

4 Design of Power Drivers

4.1 Specifications of Power Drivers

The specifications of the power driver are mainly determined by the rest of the system. First, the efficiency of the power drivers must be as high as possible in order to minimize the power dissipation and maximize the time between recharge of the device. The frequency is chosen to support a high enough data rate on the uplink direction (AM to CM) to be able to stream out all data from up to 8 NMs ($datarate = 8NM * 64channels/NM * 16kbps/channel = 8Mbps$). The output power is determined by the various configurations and operating modes of the NMs, as discussed previously. The minimum power required, ignoring the trivial case of $0\,\mathrm{mW}$, is equal to $2\,\mathrm{mW}$ and corresponds to a configuration with no NMs connected. The maximum power is determined by a configuration with 4 NMs stimulating and recording on all possible channels and is equal to about $14\,\mathrm{mW}$. Another way to interpret this variable power range, assuming a constant-voltage source, is to calculate the equivalent load that the power drivers must drive. Assuming that the output voltage of the power drivers is

$$V_{out,pp} = 3.3V,$$

we can calculate an equivalent resistance for the AM load R_{AM}, NM load R_{NM}, and equivalent load of the power drivers $R_{eq} = R_{AM}||R_{NM1}||R_{NM2}||...$ for both the minimum and maximum output power with the following:

$$R = V^2/P.$$

These equivalent resistances are useful when designing power drivers and are summarized in Table 4.1 along with the rest of the power driver specifications.

4.2 Differential Power Delivery

The miniaturization of the implanted devices and cables discussed in Chapter 2 allows an unprecedented number of neural interfaces to be implanted in the brain without significant tissue damage, but this shrinking of interconnects and devices poses a challenge for data communications. In the

Specification	**Minimum**	**Maximum**
Frequency	$20\,\mathrm{MHz}$	$20\,\mathrm{MHz}$
Output power	$2\,\mathrm{mW}$	$14\,\mathrm{mW}$
R_{AM}	$5.4\,\mathrm{k\Omega}$	$5.4\,\mathrm{k\Omega}$
R_{NM}	$3.6\,\mathrm{k\Omega}$	∞
R_{eq}	$0.8\,\mathrm{k\Omega}$	$5.4\,\mathrm{k\Omega}$

Table 4.1: Specifications for the design of the differential AC power drivers.

case of OMNI, the main challenge is minimizing cross-coupling between data-to-data and power-to-data wires inside the small cable bundle. The cable bundle utilized for OMNI is meant to be thin and flexible enough to allow surgeons to place a NM anywhere on the brain and easily connect to the AM, so the cable thickness and inter-cable distance is minimized in order to optimize cable flexibility and size. Unfortunately, this cable design results in large electrical resistances (up to $20\,\Omega$) and more importantly large parasitic capacitances between cable wires (a few pF per cm). These inter-wire capacitances not only load the power drivers, but also lead to significant signal coupling between wires which can corrupt data and lead to device failure. In the case of OMNI, cross-talk between wires is a major problem. The data link is designed for low power and operates at $1.2\,\mathrm{V}$, while the AC power signals must be at a relatively higher voltage - $3\,\mathrm{V}$ to $4\,\mathrm{V}$ - in order to operate the NMs efficiently. Based on the design of the data link receivers (not covered in detail in this work), the worst case cross-talk that could be tolerated without corrupting data is $200\,\mathrm{mV}$. This means that cross-talk between power and data of only 5% will corrupt the data signal. This cross-talk problem was extensively studied from the perspective of the physical cable design, but procuring medical grade cables that met our specifications in terms of size, resistance, capacitance, and flexibility proved to be too expensive. Thus, we chose to minimize cross-talk by utilizing a symmetrical cable design and differential power signals.

Figure 4.1 shows simulation waveforms for three different cable and signaling designs. In each case, the AC power signals are +/- $3.6\,\mathrm{V_{pp}}$ while the data signals are $1.2\,\mathrm{V}$ in amplitude, and only the physical parameters of the cable model and the power signaling scheme was changed. The green trace is the data signal at the driver while the yellow, red, and blue traces are the received data signals on the other side of the cable for the three configurations. The red trace corresponds

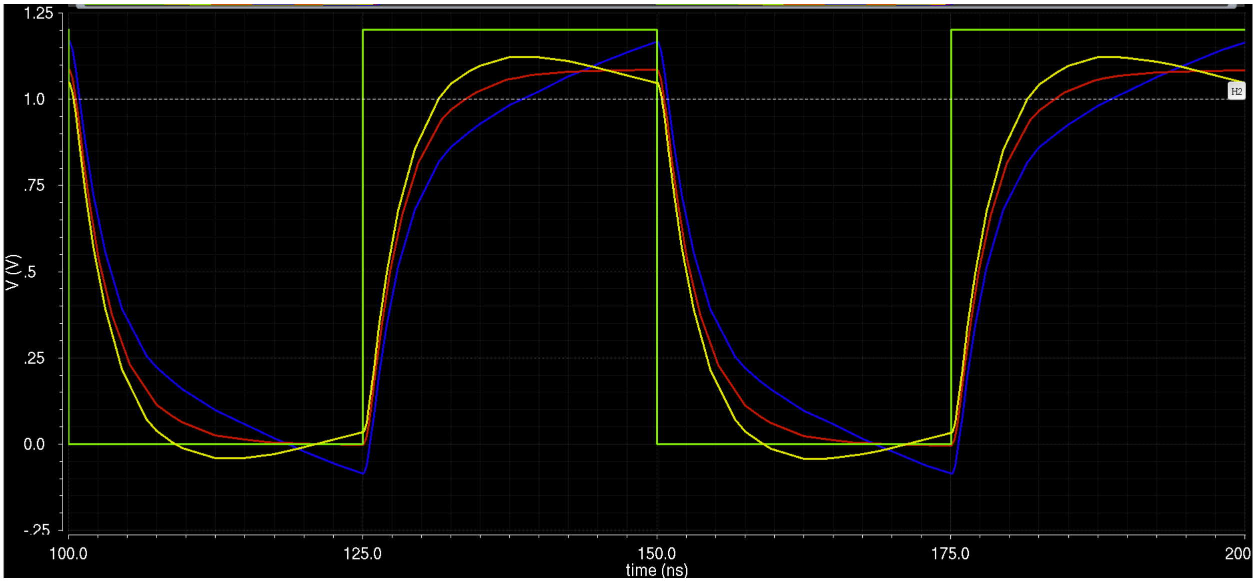

Figure 4.1: Simulation results of power-data cross-talk for three different cable and AC power signaling configurations. The green waveform is the data input bit stream, while the yellow, red, and blue signals are the received data signal at the other end of the wire. When utilizing differential power signaling and symmetric cable design, cross-talk between power and data lines can be minimized.

to a configuration in which the data wire has no other wires around it (no coupling), the blue trace to a configuration in which the data wire is near a single-ended $3.6\,\mathrm{V_{pp}}$ power signal, and the yellow trace shows to a configuration which has two fully differential $3.6\,\mathrm{V_{pp}}$ power signals equidistant to the data wire. The dotted horizontal white line denotes $1\,\mathrm{V}$. As can be seen, when there are no wires to couple into the data line (red), the signal can rise to a ”high” value before it is clocked by the receiver. When there is a single ended power signal (blue), this higher voltage signal can destructively couple into the data wire when there is a 180° phase shift between power and data signals, which can cause bit errors at the receiver. However, if there are two differential power signals placed equidistantly from the data wire so that their coupling is equal (yellow), the coupling from each power wire to data wire destructively interferes and cancels.

4.3 Power Driver Architecture Design

Now that the electrical specifications and physical interconnect parameters have been defined, the design of the power drivers themselves can begin. Based on the analysis of cross-talk and coupling, it was determined that the power driver must generate a pair of fully differential power signals at $20\,\mathrm{MHz}$. Because these signals are perfectly symmetrical, we can design a single power driver and create a copy that is 180^{o} out of phase. Driven by the need for very high efficiency AC power delivery, a classical Class-E power amplifier topology was selected. A Class-E amplifier can achieve a theoretical 100% efficiency by utilizing zero voltage switching (ZVS) and zero current switching (ZCS) operation [9], making it the perfect candidate for this application. Furthermore, it can be implemented reliably using only a few COTS components, requires only one active device, and can generate differential signals easily.

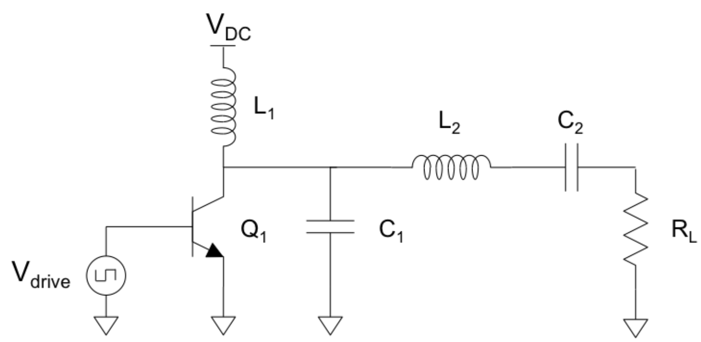

Figure 4.2: Basic schematic of a Class-E amplifier.

Figure 4.2 shows a canonical Class-E amplifier topology. The switch Q1 is driven by the fundamental frequency, effectively switching the output LC network between the supply and ground. L_1 is a big inductor acting as an RF choke. C_1 is the combination of shunt capacitance from L_1, the output capacitance of the switch, wiring capacitance, and any physical capacitor inserted in order to shape the output waveform. L_2 and C_2 form the resonant tank at the required frequency. Finally, the resistor R_L represents the load that the amplifier must drive.

Unfortunately, Class-E amplifiers are typically designed to provide a fixed amount of power (or gain). From the discussion in Chapter 3, it is clear that OMNI's load is not fixed, but varies by an order of magnitude. Thus, we must make some modifications to the canonical Class-E amplifier in order to provide the correct voltage and power at the AM and NMs.

There are two more interesting features of the Class-E topology, outlined below.

1. The output voltage is (almost) linearly dependent on the supply voltage. In other words, in order to increase output voltage, and in turn output power, we can increase the supply voltage directly.

2. The output frequency is mainly determined by the frequency of the gate drive and the LC tank. We can use the gate drive in order to tune the driver to a particular frequency and the LC tank to tune out the load parasitics and harmonics. This is crucial for the AM and NMs since they recover their clocks directly from these power signals.

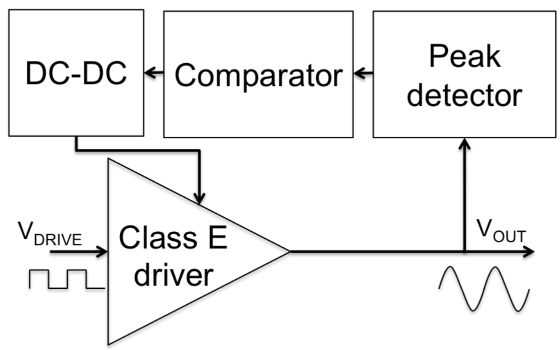

Figure 4.3: Circuit architecture for an adaptable, constant-voltage AC power driver based on a Class-E amplifier and voltage feedback loop.

Figure 4.3 shows the proposed circuit architecture for an adaptable constant-voltage AC power driver. The main components are the traditional Class-E power amplifier, a peak detector, and a voltage-controlled DC-DC regulator. The basic operation can be described as follows:

1. The Class-E switch is driven by a $20\,\mathrm{MHz}$ square wave generated with an FPGA which generates a sinusoidal output signal at the correct desired frequency. This gate drive is also responsible for ensuring that the two power signals are completely out of phase.

2. The peak detector senses the peak voltage of the AC waveform and compares it to a reference voltage using a high speed op-amp.

3. This op-amp drives the feedback terminal of the DC-DC regulator, setting its DC voltage such that the output of the power amplifier is close to $3.6\,\mathrm{V_{pp}}$.

The following sections describe the sub-blocks in more detail.

4.3.1 Class-E Amplifier

The Class-E amplifier utilizes an NXP BFS20 npn transistor for its low collector capacitance of $1\,\mathrm{pF}$ and high speed of $450\,\mathrm{MHz}$. This switch drives an LC tank that resonates out any harmonics and ensures that the output frequency is precisely $20\,\mathrm{MHz}$. The output network is designed such that the amplifier operates with ZVS and maximum efficiency. Simulation results of this Class-E amplifier can be seen in Figure 4.4, which shows the waveforms at the gate, drain, and output of the Class-E amplifier. The designed Class-E operates with ZVS and achieve an efficiency of 91% in this particular configuration.

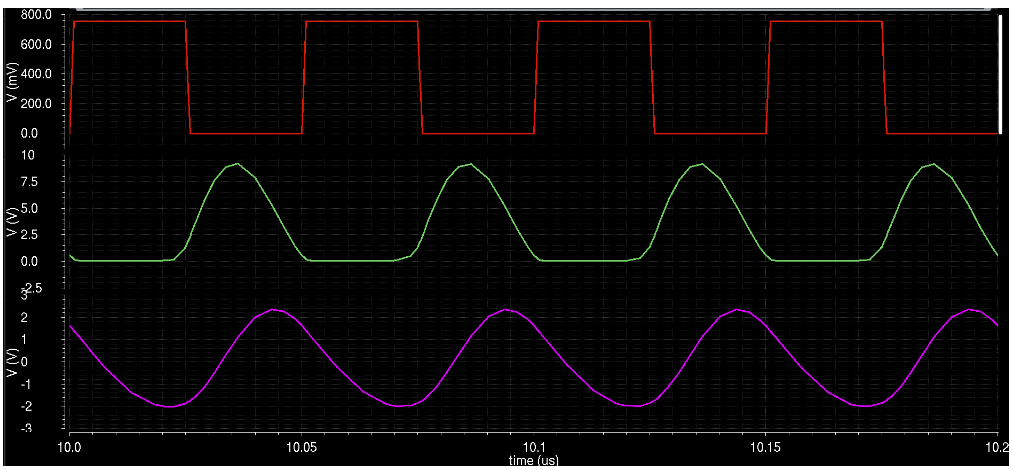

Figure 4.4: Circuit simulation for the designed Class-E power amplifier. The gate is driven by a $20\,\mathrm{MHz}$ square wave (red), which generates a ZVS signal at the drain of the switch (green) and a $20\,\mathrm{MHz}$ output voltage signal (purple). Note that the output voltage amplitude in this simulation was not designed to be $3.6\,\mathrm{V_{pp}}$.

4.3.2 Peak Detector

The peak detector consists of a Texas Instruments OPA2889 op-amp in voltage-follower configuration to buffer the AC signal and minimize parasitic loading. The OPA2889 has an input capacitance of 0.5pF and is negligible compared to the capacitance of the cables and load. The rectification is done by a Diodes SDM02 Schottky diode with a low forward voltage drop of 0.2V that helps maximize efficiency.

4.3.3 Comparator and DC-DC Regulator

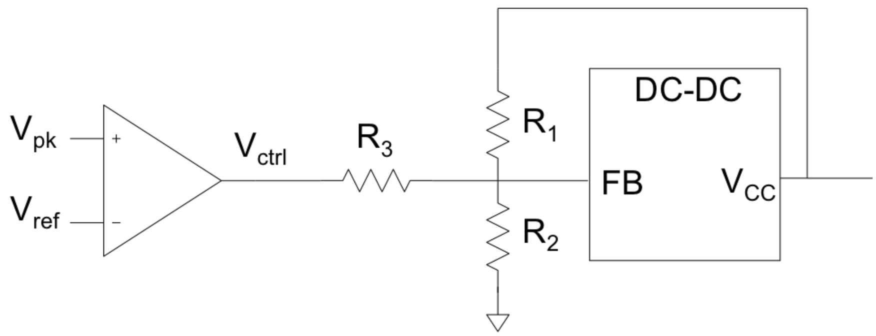

Figure 4.5: Detailed circuit diagram of comparator and DC-DC regulator portions of power drivers showing part of the feedback network that sets a constant output voltage.

The DC-DC regulator is a Texas Instruments TPS63030 buck-boost converter operating with resistive feedback as shown in Figure 4.5. An OPA2889 op-amp is utilized to compare the rectified output voltage V_{pk} of the Class-E amplifier and compare it to a DC reference V_{ref} in order to generate a control signal, V_{ctrl}. This signal drives the resistive feedback network made up of R_1, R_2, and R_3 in order to set the output DC-DC voltage (and Class-E supply voltage) V_{CC}. By modulating the supply voltage of the Class-E, this feedback loop ensures that the output voltage of the Class-E remains constant, with a peak value determined by V_{ref}.

The output voltage V_{CC} of the DC-DC can be expressed as

$$V_{CC} = 0.5\,\mathrm{V} * (1 + R_1/R_2 + R_1/R_3) - V_{ctrl} * R_1/R_3,$$

where the $0.5\,\mathrm{V}$ is determined by the DC-DC's internal reference voltage. In order to achieve the full range of output voltages for the DC-DC given the maximum range of V_{ctrl}, the three resistors are chosen based on the following system of equations:

$$V_{CC,min} = 0.5\,\mathrm{V} * (1 + R_1/R_2 + R_1/R_3) - V_{ctrl,max} * R_1/R_3,$$

$$V_{CC,max} = 0.5\,\mathrm{V} * (1 + R_1/R_2 + R_1/R_3) - V_{ctrl,min} * R_1/R_3.$$

The minimum and maximum output voltages for the DC-DC and OPA2889 are taken directly from their datasheets:

$$V_{CC,min} = 1.2\,\mathrm{V},$$

$$V_{CC,max} = 5.5\,\mathrm{V},$$

$$V_{ctrl,min} = -4\,\mathrm{V},$$

$$V_{ctrl,max} = 4\,\mathrm{V}.$$

In order to solve this system of equations (2 equations, 3 unknowns), we choose a value for $R_2 = 200\,\mathrm{k\Omega}$ in order to set the divider current at $2.5\,\mathrm{\mu A}$. Using these values, we can solve for the values of R_1, R_3, $V_{CC,min}$, and $V_{CC,max}$. The final results are summarized below.

$$R_1 = 1030\,\mathrm{k\Omega},$$

$$R_2 = 200\,\mathrm{k\Omega},$$

$$R_3 = 1920\,\mathrm{k\Omega},$$

$$V_{CC,min} = 0.5\,\mathrm{V} * (1 + 1030\,\mathrm{k\Omega}/200\,\mathrm{k\Omega} + 1030\,\mathrm{k\Omega}/1920\,\mathrm{k\Omega}) + 4\,\mathrm{V} * 1030\,\mathrm{k\Omega}/1920\,\mathrm{k\Omega} \approx 5.49\,\mathrm{V},$$

$$V_{CC,max} = 0.5\,\mathrm{V} * (1 + 1030\,\mathrm{k\Omega}/200\,\mathrm{k\Omega} + 1030\,\mathrm{k\Omega}/1920\,\mathrm{k\Omega}) - 4\,\mathrm{V} * 1030\,\mathrm{k\Omega}/1920\,\mathrm{k\Omega} \approx 1.20\,\mathrm{V}.$$

Unfortunately, few simulation models are available for the COTS components used in this design, which makes simulating the entire feedback loop difficult. The DC-DC regulator and op-amp have no reliable models available from the manufacturers, while the SPICE models provided for the Schottky diodes used in the peak detector of the CM and the rectifier on the AM are inaccurate. To address this, we developed rudimentary models of the above components using device datasheets and benchtop measurements which were sufficient to demonstrate proper operation of the circuit.

4.4 Adaptability of Power Drivers to Changes in Load

Figure 4.6a shows the simulation setup used to determine the power driver's adaptability to changes in load. A variable load resistor ($500\,\Omega$ to $6000\,\Omega$) was used to simulate the variable loading of an AM and 0-4 NMs as outlined in Chapter 4.1. The reference voltage fed to the peak detector block was set such that the peak-to-peak voltage of the output AC waveform is $3.3\,\mathrm{V}$. The Class-E amplifier was designed to achieve maximum efficiency for a nominal load of $1.5\,\mathrm{k\Omega}$, which is meant to represent a typical use case for OMNI. As can be seen in Figure 4.6b, the feedback loop maintains a stable voltage across almost the entire range of loads. Figure 4.6c shows the efficiency and output power of the power driver across this load variation, which shows that the output power can range from $1.77\,\mathrm{mW}$ to $21.0\,\mathrm{mW}$ while maintaining efficiencies greater than 73%.

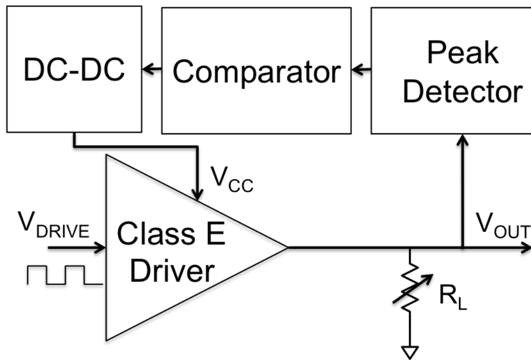

(a)

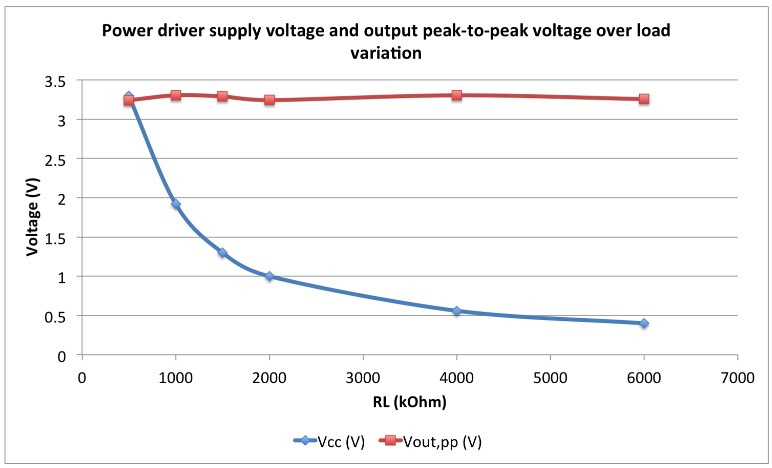

(b)

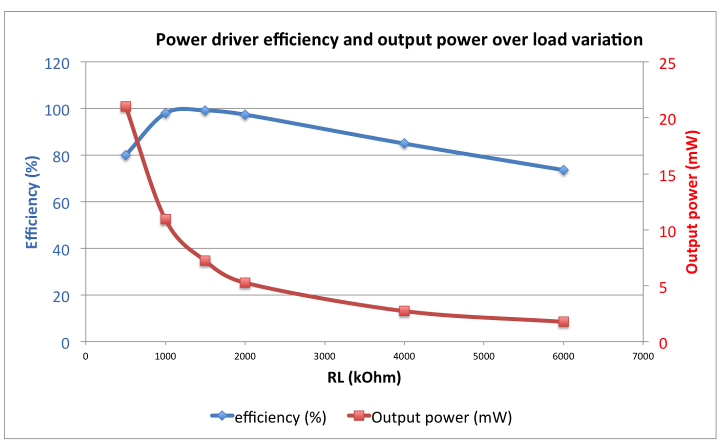

(c)

Figure 4.6: (a) Simulation setup for verifying power drivers adaptability to load variation. (b) Supply voltage varies with load in order to set a constant output peak-to-peak voltage of $3.3\,\mathrm{V}$. (c) Efficiency and output power over load variation showing efficiency variation as the load moves farther away from its nominal value of $1.5\,\mathrm{k\Omega}$.

5 Experimental Results

In order to verify the operation of the OMNI system, several testbeds were created. All parts of OMNI were extensively tested and shown to perform to the designed specifications, including the recording and stimulation capabilities of the NMs, the custom communication protocol between NMs, AM, and CM, and the wireless link between CM and GUI. The test setup used for this verification is shown in Figure 5.1. It shows two NMs on breakout boards, an AM on its breakout board, and the CM all connected using Omnetics cables adapted to our custom 6-wire interface. DC power for the CM comes from a benchtop supply and the CM generates the AC waveforms required to power the rest of the system as discussed in the previous chapter.

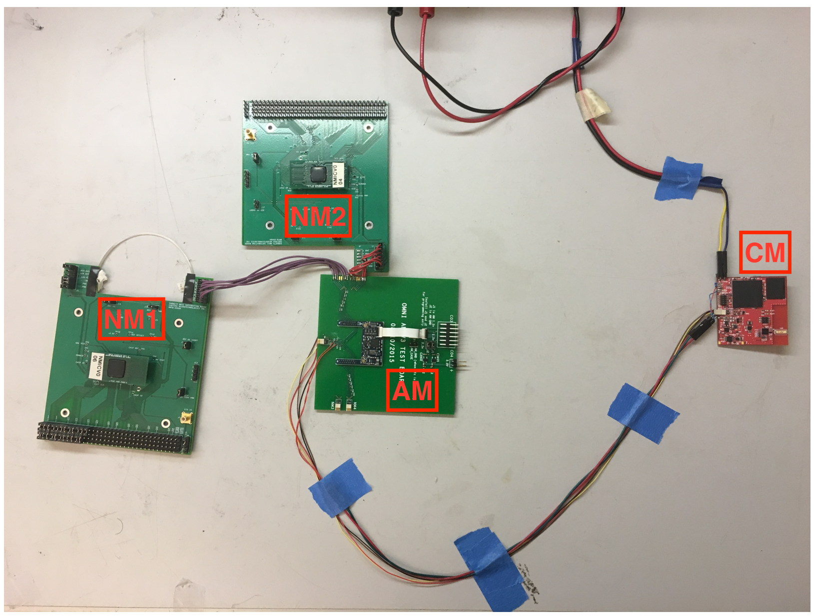

Figure 5.1: Benchtop test setup for verifying functionality of OMNI.

To test the power drivers, two testboards were built and are shown in Figure 5.2. In order to accurately account for parasitic effects on the final Class-E circuit, an exact replica of the power driver circuits were laid out side-by-side on a small testboard (Figure 5.2a), mirroring the final layout and form factor of the circuit on the CM board. This ensures that any parasitic capacitances introduced at sensitive nodes of the circuit (e.g. the drain of the active device) do not significantly change the operating point on the CM. Unfortunately, the small form-factor of this board makes incremental testing a challenge, so a second testboard (Figure 5.2b) was designed in order to explore and characterize various features of the power drivers.

The testboard in Figure 5.2b includes test loads for the AM and up to 4 NMs, modeled using a full wave diode bridge utilizing low forward voltage drop Schottky diodes for the RF-to-DC and a potentiometer for the DC load. Individual NMs can be connected and disconnected through pairs of jumpers, allowing the power driver circuit to be tested under all possible load conditions easily. The power driver circuit itself consists of the Class-E amplifier and feedback network, as well as pads where a 6-wire cable can be attached in order to verify that the data link remains uncorrupted due to cross-talk while driving the AM/NM loads.

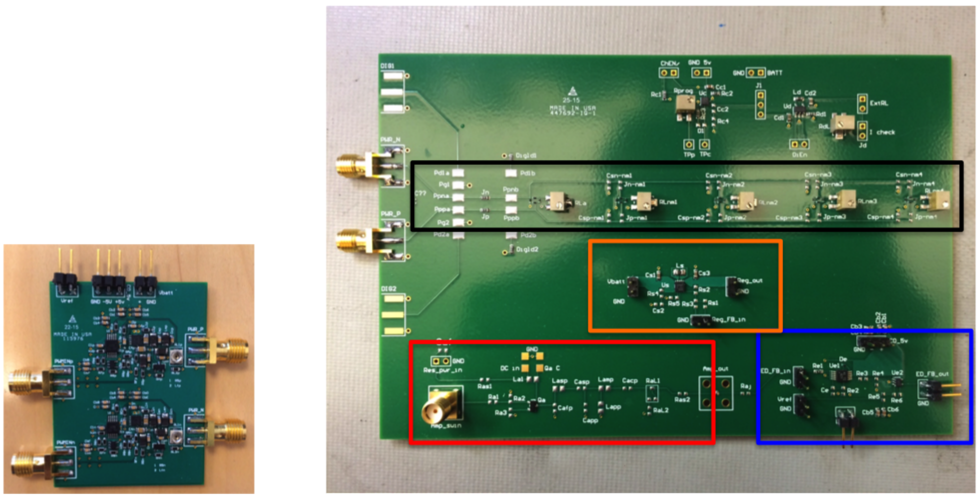

(a) (b)

Figure 5.2: (a) Power driver testboard with same footprint as final CM board to replicate parasitics. (b) Expanded power driver testboard with Class-E power amplifier (red), peak detector (blue), DC-DC regulator (orange), and adjustable AM and NM loads (black).

A major challenge in measuring the performance of the power drivers was the inability to accurately display the drain waveform of the Class-E amplifier. As discussed in Chapter 4, maximum efficiency of a Class-E is realized through ZVS at the drain. This ZVS condition is achieved by properly sizing the capacitors C_1 and C_2 based on the shape of the voltage waveform at the drain of the switch. When measuring this voltage, care must be taken to not perturb the characteristics of the Class-E amplifier itself via capacitive loading from the probe. In our circuit, the capacitance at this node is on the order of $3\,\mathrm{pF}$ and any probe loading capacitance must be much smaller than this, preferably on the order of fF. A standard passive probe such as the Tektronix P6139A or Agilent N2890A has an input capacitance of $8\,\mathrm{pF}$ and $11\,\mathrm{pF}$, respectively, and would detune the circuit significantly, so an active high-speed probe is required. The high speed probe used has an input capacitance of $500\,\mathrm{fF}$, but a maximum input voltage of only $4\,\mathrm{V}$. Unfortunately, the peak voltage at the drain is on the order of $4V_{\mathrm{dd}}$ and can reach up to $20\,\mathrm{V}$, saturating the probe amplifier, distorting the waveform, and making tuning difficult. As a result of this, the power drivers were not easily tuned for maximum efficiency and this metric is not measured. Nonetheless, taking into account the overall efficiency of the feedback network and board parasitics, the maximum efficiency is estimated to be close to 70%.

Figure 5.3 shows transient waveforms captured on an oscilloscope of a single channel of the power driver. The $20\,\mathrm{MHz}$ square wave signal is generated by a function generator and fed into one input port of the testboard shown in Figure 5.2a. The sine wave is the measured output when driving a $2\,\mathrm{k\Omega}$ load. This setup was replicated with a varying load and the results are shown in Figure 5.4. As can be seen, the power driver circuit is able to drive a wide range of loads ($400\,\Omega$ to $5000\,\Omega$) while maintaining a steady output voltage.

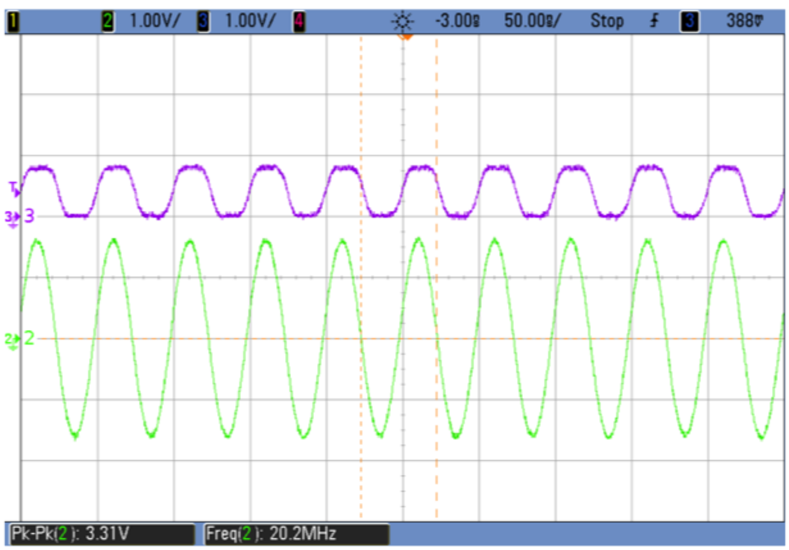

Figure 5.3: Measured input and output waveforms of a single-ended power driver driving a $2\,\mathrm{k\Omega}$ load.

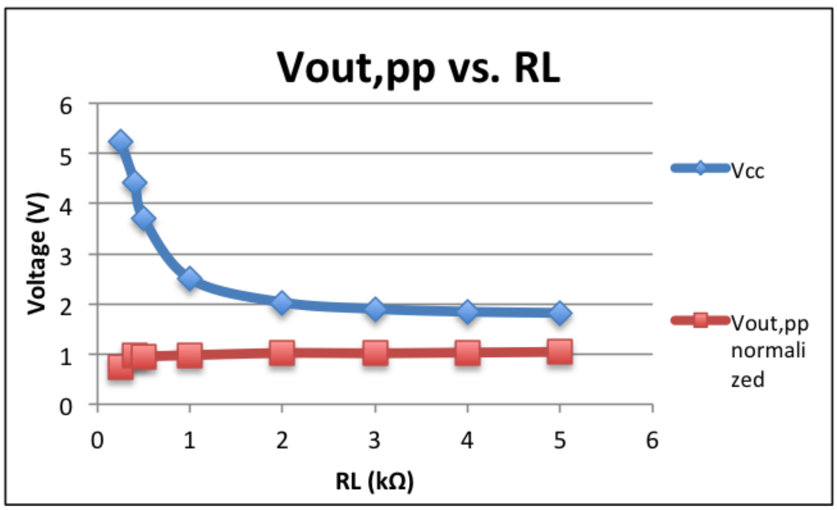

Figure 5.4: Measured V_{CC} and $V_{out,pp}$ voltages for power driver driving a variable load.

6 Conclusions and Future Work

This work presented OMNI, a distributed and modular neuromodulation device for studying and treating a wide array of neurological conditions. OMNI includes support for up to 256 channels of simultaneous recording and stimulation on up to 16 independent channels using fully configurable stimulators. The unique architecture of OMNI allows neurosurgeons to reach physically distant regions of the brain with one system and only a few implanted modules. Additionally, OMNI includes a Control Module that is responsible for power management and distribution, processing, data logging, and telemetry for wireless data transmission. OMNI's design offers the capability to address disorders presented at the network level and enables a new class of closed-loop neuromodulation therapis.

This thesis focused on the challenge of powering such a distributed and implanted medical system. The order-of-magnitude variation in loading caused by the modularity of OMNI, combined with medical implant regulations that require implanted wires to carry no DC component make powering the sub-modules of OMNI a difficult problem. This work presents one solution to this problem which uses fully differential Class-E power drivers with an adaptive feedback network to produce a constant output voltage across load variations. A prototype power driver circuit was designed, built, and tested *ex vivo* in order to show functionality of the power distribution scheme. This circuit was then implemented on the final OMNI system in order to create a fully implantable and wireless system for closed-loop neuromodulation.

The next steps in improving the OMNI system as a whole is to further improve the robustness and efficiency of the power drivers across various load conditions. In this first prototype, the power drivers can only adjust their output voltage in response to a change in DC load. While this is enough to ensure the correct power is transmitted to the AM and NMs, it decreases the efficiency of the power drivers since they are no longer operating under the ideal, ZVS condition they were designed for. In order to address this, a tunable output LC network or adaptive gate drive can be implemented in order to ensure the active device in the Class-E amplifiers operates with ZVS.

Another improvement to the power distribution network will be output voltage sensing at the end points instead of the origin of the power signals. Currently the output voltage amplitude is sensed at the output of the power drivers in order to minimize the number of implanted wires required. A better sensing scheme for the feedback network would sense this amplitude at the AM and NMs, which could digitize these signals and send information back towards the CM on the existing bi-directional data lines. This back-telemetry would require slight redesigns of the AM and NMs, as well as the digital communication protocol and power driver feedback networks, but would drastically improve the dynamic behavior of the power drivers.

The power drivers designed and discussed in this work can provide reliable and safe power to all sub-modules of OMNI and bring us one step closer to realizing a chronic, wireless device capable of performing closed-loop neuromodulation therapies to potentially address debilitating conditions like depression, anxiety, and stress.

Bibliography

[1] W. H. Organization, *Neurological disorders: public health challenges*. World Health Organization, 2006.

[2] R. C. Kessler, W. T. Chiu, O. Demler, and E. E. Walters, "Prevalence, severity, and comorbidity of 12-month dsm-iv disorders in the national comorbidity survey replication," *Archives of general psychiatry*, vol. 62, no. 6, pp. 617–627, 2005.

[3] D. Blumer, G. Montouris, B. Hermann, *et al.*, "Psychiatric morbidity in seizure patients on a neurodiagnostic monitoring unit," *Journal of Neuropsychiatry and Clinical Neurosciences*, vol. 7, no. 4, pp. 445–456, 1995.

[4] S. Stanslaski, P. Afshar, P. Cong, J. Giftakis, P. Stypulkowski, D. Carlson, D. Linde, D. Ullestad, A.-T. Avestruz, and T. Denison, "Design and validation of a fully implantable, chronic, closed-loop neuromodulation device with concurrent sensing and stimulation," *Neural Systems and Rehabilitation Engineering, IEEE Transactions on*, vol. 20, no. 4, pp. 410–421, 2012.

[5] F. T. Sun and M. J. Morrell, "The rns system: responsive cortical stimulation for the treatment of refractory partial epilepsy," *Expert review of medical devices*, vol. 11, no. 6, pp. 563–572, 2014.

[6] C. Hammond, R. Ammari, B. Bioulac, and L. Garcia, "Latest view on the mechanism of action of deep brain stimulation," *Movement disorders*, vol. 23, no. 15, pp. 2111–2121, 2008.

[7] J.-P. Langevin, A. A. De Salles, H. P. Kosoyan, and S. E. Krahl, "Deep brain stimulation of the amygdala alleviates post-traumatic stress disorder symptoms in a rat model," *Journal of psychiatric research*, vol. 44, no. 16, pp. 1241–1245, 2010.

[8] H. S. Mayberg, A. M. Lozano, V. Voon, H. E. McNeely, D. Seminowicz, C. Hamani, J. M. Schwalb, and S. H. Kennedy, "Deep brain stimulation for treatment-resistant depression," *Neuron*, vol. 45, no. 5, pp. 651–660, 2005.

[9] N. O. Sokal and A. D. Sokal, "Class e - a new class of high-efficiency tuned single-ended switching power amplifiers," *Solid-State Circuits, IEEE Journal of*, vol. 10, no. 3, pp. 168–176, 1975.